INSTITUTE OF PHYSICS PUBLISHING JOURNAL OF PHYSICS: CONDENSED MATTER

J. Phys.: Condens. Matter **16** (2004) S455–S470 PII: S0953-8984(04)68820-5

Recent developments in hard magnetic bulk materials

Josef Fidler, Thomas Schrefl, Sabine Hoefinger and Maciej Hajduga

Institute for Solid State Physics, Vienna University of Technology, Wiedner Hauptstrasse 8–10, A-1040 Wien, Austria

E-mail: fidler@tuwien.ac.at

Received 10 September 2003
Published 23 January 2004
Online at stacks.iop.org/JPhysCM/16/S455 (DOI: 10.1088/0953-8984/16/5/007)

Abstract

The importance of newly developed permanent magnetic materials in many electromechanical, magnetomechanical and electronic applications is attributed to the drastic improvement in microstructure related properties, such as the remanence, the magnetic energy density product and the coercive field. The influence of the microstructure on the magnetic properties of the magnets will be discussed, where special emphasis is laid on rare earth permanent magnets. Highest performance, anisotropic Nd–Fe–B magnets with $J_r > 1.5$ T, $(BH)_{max} > 450$ kJ m^{-3} and $_JH_c > 750$ kA m^{-1}, which are produced by the powder metallurgy route, show a strong influence of composition and processing parameters on the magnetic properties. The magnetic properties of $Sm(Co, Cu, Fe, Zr)_z$ sintered magnets, which are used nowadays for high temperature applications between 300 and 500 °C, are determined by the cellular precipitation microstructure, which is developed during a complex heat treatment and by the microchemistry. Special hard magnetic powder materials, such as $Sm_2Fe_{17}N_3$ and nanocrystalline, composite $Nd_2Fe_{14}B/(\alpha\text{-Fe}, Fe_3B)$ materials have been developed especially for usage in bonded magnetic materials, which show the strongest annual increase in the production of permanent magnets. The phenomenon of the enhancement of remanence, occurring in single phase and composite $Nd_2Fe_{14}B$ based magnets with isotropic grain alignment, is attributed to intergrain exchange interactions.

1. Introduction

The history of permanent magnetism reaches back to ancient Greece, where the ability of the loadstone to attract iron was discovered. The modern history of permanent magnetic materials starts at the end of the century before last with the development of special alloy steels. The intrinsic coercivity and the energy density product of such magnetic steel materials were rather low compared to those of recently developed hard magnetic materials. The magnetic hardness of permanent magnet materials depends critically on the microstructure

of the individual magnets. In the light of the historical development of the coercive field and the energy density product of hard magnetic materials the improvement of the energy density product is closely connected with a better understanding of the mechanisms leading to higher coercive forces of the magnets [1–4]. High external magnetic fields are necessary to obtain saturation in permanent magnets, unlike the case for soft magnetic materials, which are saturated by relatively low magnetic fields. Permanent magnets should exhibit a magnetic field after saturation regardless of external fields. The only functions of a permanent magnet are providing an external field and creating free magnetic poles in an air gap. The resulting magnetic field in the air gap H_{ag} is directly proportional to the volume of the magnet V_m and the stored energy density product $(B_m H_m)$, according to

$$H_{ag} \approx \sqrt{\frac{V_m(B_m|H_m|)}{\mu_0 V_{ag}}}. \tag{1}$$

A magnet should be shaped for the most efficient use in such a way that its operating point is close to the $(BH)_{max}$ point. It is evident that increase of the energy density product reduces, besides the volume, also the weight of the permanent magnet containing device and that new static field designs, such as charged beam guiding systems and dynamic devices, are possible.

Besides the Curie temperature and the energy density product, the remanence that determines the maximum flux density within the air gap of a magnetic circuit and the coercive field are also necessary to distinguish and describe different permanent magnet materials. The coercive field determines the magnetic 'hardness' against external magnetic fields. For practical applications the temperature coefficients of the remanence and the coercive field are also important parameters, which considerably vary in different types of magnet. Rare earth intermetallic phases with a high uniaxial magnetocrystalline anisotropy, such as $SmCo_5$, Sm_2Co_{17} and $Nd_2Fe_{14}B$, are the basis for high performance rare earth magnets [5–8]. Samarium–cobalt magnets exhibit the highest coercive fields ${}_JH_c$ and $Nd_2Fe_{14}B$ based magnets show the highest value of the remanence B_r and energy density product $(BH)_{max}$ obtained so far. Rare earth magnets are divided into the group of the so-called single phase, nucleation controlled magnets, based on the $SmCo_5$ or $Nd_2Fe_{14}B$ hard magnetic phases, and the group of domain wall pinning controlled, multiphase magnets. Two phase magnets, which are nowadays also used in high temperature advanced power applications, consist of a continuous $Sm(Co, Cu)_{5-7}$ cellular precipitation structure within a $Sm_2(Co, Fe)_{17}$ matrix phase. Nanocrystalline rare earth magnets exhibit microstructures of single phase, two phase and multiphase character, in which the inhomogeneous magnetization behaviour near the intergranular regions creates remanence enhancement.

A combination of the intrinsic properties of the material, such as the saturation polarization J_s, magnetic exchange and magnetocrystalline anisotropy of various phases, and the influence of the microstructure on the magnetization reversal process govern the hysteresis properties of the magnets. The intergranular structure between the grains plays a significant role in determining the magnetic properties; thus a detailed understanding of the microstructure and grain boundaries is necessary. The microstructural features directly influence magnetic domain structures, which are a result of the occurrence of magnetic stray fields. The direct observation of microstructure and magnetic domain structure leads to a deeper insight into the reasons for the coercivity of rare earth magnets. Advanced analytical methods, such as high resolution electron microscopy, force microscopy and position sensitive 3D atom probing, have been used to study rare earth magnets. Modelling of magnetic materials is performed at various levels and becomes more important as computer power is improved. Numerical 3D micromagnetic simulations of the magnetization reversal process nowadays incorporate realistic microstructures. Advanced analytical investigations and future simulations should

Table 1. Hard magnetic properties of commercially available permanent magnets.

Magnet	B_r (T)	${}_JH_c$ (kA m^{-1})	$(BH)_{max}$ (kJ m^{-3})	T_C (°C)
Hard ferrites	0.35	320	25	450
$AlNiCo_5$	1.30	65	60	850
$AlNiCo_8$	0.85	145	55	850
$SmCo_5$	0.90	3500	200	720
$SmCo_5/Sm_2Co_{17}$	1.15	3000	260	820
$Nd_2Fe_{14}B$	1.52	1500	450	310

be able to predict optimal microstructures and properties for given hard and soft magnetic materials [9].

2. Classification and markets for modern hard magnets

The new hard magnetic materials based on rare earth intermetallic compounds exhibit a considerably higher coercive force and energy density product than the traditional AlNiCo alloys and hard ferrites. In the late 1960s high magnetocrystalline anisotropy, the basis for a good permanent magnet material, was discovered in the USA under the leadership of Strnat [5] in several rare earth–cobalt intermetallic compounds. Soon it was discovered that the combination of the high magnetic moments of iron and/or cobalt with the high magnetic moments of heavy rare earths leads to high magnetocrystalline anisotropy and retains the high magnetic ordering temperature particularly in the system Sm–Co. The rare earth permanent magnets were discovered in the USA, but recent developments in this field have come from Japan, especially with the invention of rare earth–iron based permanent magnets, having the best magnetic properties so far achieved. In 1984 Sagawa *et al* [6], Croat *et al* [7] and Hadjipanayis *et al* [10] reported on a magnet material, based on a $Nd_2Fe_{14}B$ compound, with an energy density product of 300 kJ m^{-3}. Modern hard magnetic materials are divided into the group of conventional metallic and oxide magnets and the group of magnets based on intermetallic compounds of rare earth elements with cobalt and/or iron. Table 1 summarizes the hard magnetic properties (the remanence, the intrinsic coercive field, the energy density product and the Curie temperature) of commercially available permanent magnet materials. The $Nd_2Fe_{14}B$ based magnets with the highest energy product exhibit the lowest Curie temperature.

The powder metallurgical sintering route is the most important preparation technique for rare earth permanent magnets and consists of the following production steps:

- melting of the alloy under vacuum;
- crushing;
- milling;
- alignment in a magnetic field;
- pressing;
- sintering, annealing;
- machining, coating;
- magnetizing.

The total world production of permanent magnets is of the order of 250.000 tons per year with an annual growth rate between 10% and 20%. The world market, in value, is shared between the low cost hard ferrites (55%), the Nd–Fe–B based magnets (25%), the SmCo magnets (10%) and the AlNiCo magnets (10%). The highest increase per year is obtained in metallic and bonded Nd–Fe–B based magnets. Half of the world production of sintered

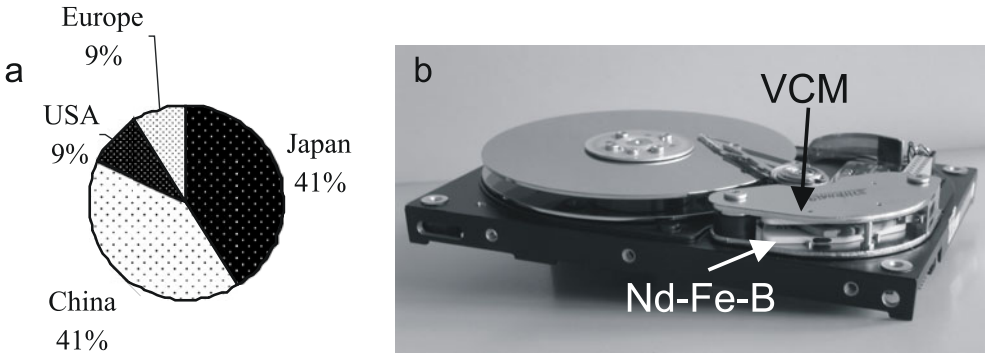

Figure 1. Sintered Nd–Fe–B magnets. (a) Average annual world production and (b) a computer hard disk showing the VCM, as a typical example of an application of Nd–Fe–B magnets.

$Nd_2Fe_{14}B$ based magnets is used in voice coil motors (VCM) in hard disk drives (figure 1(b)). Typical other applications are found in communication devices, in magnetic resonance imaging devices, in motors/generators up to a power of several megawatts for wind generators and in acoustics. The largest producers of sintered Nd–Fe–B magnets—a total of about 17 000–20 000 tons per year—are located in Japan and China, followed by the USA and Europe (figure 1(a)).

Generally permanent magnets are mainly used for:

- the storage and transformation of energy:

  mechanical energy $\rightarrow$ electric energy (microphone, generator);
  electric energy $\rightarrow$ mechanical energy (loudspeaker, motor);
  magnetic energy $\rightarrow$ mechanical energy (coupling, bearing);

- the guidance of charged particles: hexapoles, travelling wave tubes, magnetron sputtering.

The drastic increase in the energy density product of newly developed hard magnetic materials enabled the invention of many new applications of permanent magnets. Magnetic circuits, containing permanent magnets, have to be redesigned for each different magnet material. The optimum operating point which should be close to the $(BH)_{max}$ point varies for different magnet materials and magnetic circuit designs.

3. Nucleation controlled rare earth magnets

The coercive field for $SmCo_5$ and $Nd_2Fe_{14}B$ based magnets is determined by the high uniaxial magnetocrystalline anisotropy as well as the magnetostatic and exchange interactions between neighbouring hard magnetic grains. The long range dipolar interactions between misaligned grains are more pronounced in large grained magnets, whereas exchange coupling reduces the coercive field in small grained magnets. The basic microstructural feature of polycrystalline $SmCo_5$ or $Nd_2Fe_{14}B$ based magnets is the individual hard magnetic grain with its size, shape and orientation parameters. The ideal microstructure of the so-called single phase magnets consists of aligned single domain hard magnetic particles. Strictly speaking, in reality these magnets show a complex, multiphase microstructure with various types of intergranular phase according to their phase diagram and phase relations. The amounts of each phase and their distributions within polyphase materials are perhaps the most complex of the microstructural parameters. The occurrence of the multiphase microstructure is one of the reasons that the coercive fields of the magnets expected according to the magnetocrystalline anisotropy fields

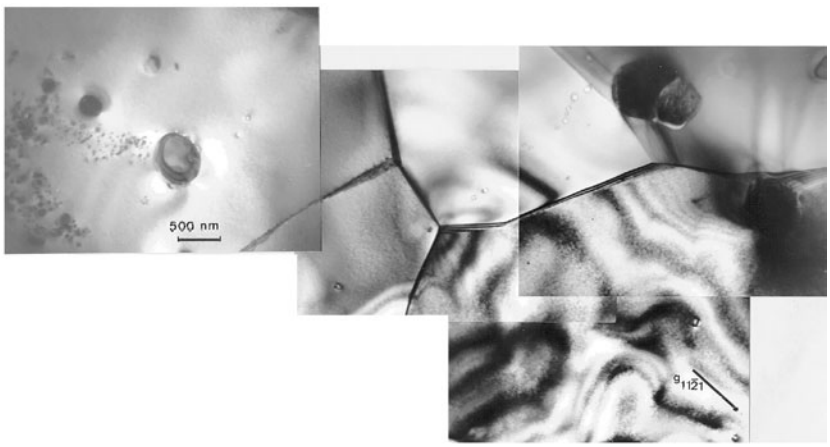

Figure 2. A TEM micrograph of a sintered $SmCo_5$ magnet showing several grains containing Sm_2O_3 and CaO inclusions. The coercivity mechanism is controlled by the nucleation and expansion of reversed domains.

of the hard phase, such as 30 700 kA m^{-1} for $SmCo_5$ and 6050 kA m^{-1} for $Nd_2Fe_{14}B$, are never reached in practice.

3.1. $SmCo_5$ magnets

The microstructure of single phase, anisotropic $SmCo_5$ type magnets consists of grains oriented parallel to the alignment direction. Most of the $SmCo_5$ grain interiors show a low defect density. The grain diameter exceeds the theoretical single domain size and is of the order of 5–10 μm. Besides $SmCo_5$ grains, grains with densely packed, parallel stacking faults perpendicular to the hexagonal *c*-axis are also observed. Such basal stacking faults correspond to a transformation of the $SmCo_5$ crystal structure into the Sm-rich Sm_2Co_7 and Sm_5Co_{19} structure types. Using high resolution electron microscopy together with x-ray microanalysis, the different polytypes and structural modifications of these Sm-rich phases are characterized. Incoherent precipitates with diameters up to 0.5 μm were identified as Sm_2O_3 or CaO inclusions. The electron micrograph of figure 2 shows several $SmCo_5$ grains with Sm_2O_3 or CaO inclusions. In $SmCo_5$ type sintered magnets the coercivity is determined by the nucleation field of reversed domains which is lower than the coercive field of a magnetically saturated particle with a single domain structure and nucleation by the expansion field of the reversed domains. The nucleation of reversed domains takes place in regions with low magnetocrystalline anisotropy. Rare earth-rich precipitates mainly degrade the ${}_JH_c$ of the final magnet. The reason for the formation of these phases is the addition of a rare earth-rich sintering aid phase before the sintering process. The coercivity can be improved by adding small amounts of transition metal powders or transition metal oxides. TEM studies show that the chemical composition, the size distribution and the impurity content (oxygen content) of the starting powder material are important factors for the magnetic properties of $SmCo_5$ type sintered magnets. For lower cost magnets, samarium is partly replaced by a mixture of cerium–mischmetal elements or, for improved magnetic properties, by praseodymium; thus three groups of $SmCo_5$ type sintered magnets are distinguished:

- (CeMM, Sm)Co_5: low J_s, $(BH)_{max}$;
- $SmCo_5$: high ${}_JH_c$;
- (Pr, Sm)Co_5: high $(BH)_{max}$.

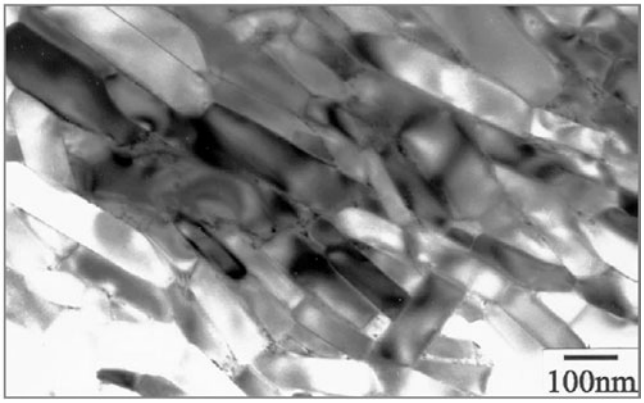

Figure 3. A TEM micrograph of a hot pressed and die-upset $Nd_{14}Fe_{72}Co_7B_6Ga1$ magnet.

Microstructural investigations on sintered magnets of the types (CeMM, Sm)Co_5 and (Pr, Sm)Co_5 showed similar results to those for $SmCo_5$ sintered magnets. The corresponding x-ray spectra of the different phases showed a mixture of rare earth elements due to their ratios of the nominal composition of the magnet.

3.2. $Nd_2Fe_{14}B$ magnets

High performance $Nd_2Fe_{14}B$ based permanent magnets are produced with different compositions and various processing techniques [11, 12], which influence the complex, multiphase microstructure of the magnets, such as the size and shape of grains, the orientation of the easy axes of the grains and the distribution of the phases. The formation and distribution of the phases are determined by the composition of the magnets and the annealing treatment. In particular, the grain size of the magnets and the alignment of the grains strongly depend on the processing parameters:

- Grain sizes in the range between 10 and 500 nm are obtained by melt-spinning, mechanical alloying and the HDDR (hydrogenation–disproportionation–desorption–recombination) process.
- Sintered and hot worked magnets exhibit grain sizes above 1 μm.

The processing route of the magnet strongly influences the grain size and grain size distribution. The coercive field in sintered magnets strongly depends on the sintering parameters, such as temperature and time. Nanocrystalline and submicron magnets are obtained by the melt-spinning route or by mechanically alloying or by the HDDR process. Hot pressing and die upsetting of Nd–Fe–B ribbon materials reveals a densely packed, anisotropic magnetic material. Platelet shaped grains with diameters less than 1 μm are observed by TEM investigations. The degree of orientation of the platelets, which are stacked transverse to the press direction with the easy *c*-axes perpendicular to the face of each grain, determines the remanence and coercive field of the magnet [13]. The degree of alignment and the size and shape of the grains and the intergranular regions within the ribbons control the macroscopic magnetic properties. Die upsetting modifies the spheroidal grains after hot pressing to platelets as shown in the TEM micrographs of figure 3. Misaligned grains, which are clearly visible, degrade the remanence. The *c*-axis for each grain runs perpendicular to the straight elongated edge. An Nd-rich phase is found among the platelet shaped grains as a fine layer between the

straight edges or as pockets at the end of the platelets or between the misaligned and aligned grains. On the other hand, the magnets with a lower remanence show a microstructure with more equiaxial grains. In most of the melt-spun magnets regions with abnormally grown, large grains were found. Some of these grains were fully developed, platelet shaped grains.

Substituent and dopant elements influence the microstructure, coercivity and corrosion resistance of advanced (Nd, S1)–(Fe, S2)–B:(M1, M2) magnets. The replacement of the Nd-rich intergranular phase by secondary phases formed after doping by M1 and M2 type elements improves the corrosion resistance, especially in large grained magnets. The multicomponent composition of the magnets leads to the formation of non-magnetic and soft magnetic phases. Generally, two types of substituent element, which replace the rare earth element or the transition element sites in the hard magnetic phase, and two types of dopant element are distinguished [14]. Substituent elements mainly change the intrinsic properties, such as the spontaneous magnetic polarization, Curie temperature and magnetocrystalline anisotropy. Depending on the type, the dopant elements, which show a low solubility within the hard magnetic phase, form additional intergranular rare earth containing or boride phases. These phases change the behaviour of the coupling between the hard magnetic grains. Non-magnetic intergranular phases eliminate the direct exchange interaction and also reduce the long range magnetostatic coupling between the hard magnetic grains; both effects lead to an increase of the coercive field. On the other hand, the decrease of the volume fraction of the hard magnetic phase within the magnet decreases the remanence. Insufficient temperature stability and poor corrosion resistance are the main factors limiting applications of $Nd_2Fe_{14}B$ based magnets. Secondary non-magnetic phases, which replace the Nd-rich intergranular phase, considerably improve the corrosion resistance and are of great technological interest.

Nd–Fe–B based permanent magnets with a composition close to $Nd_{15}Fe_{77}B_8$ exhibit a complex multiphase microstructure. According to the ternary phase diagram, at least three equilibrium phases occur:

- the hard magnetic $Nd_2Fe_{14}B$ phase;
- the boride phase $Nd_{1+\varepsilon}Fe_4B_4$;
- the low melting point Nd-rich phase.

Other phases, such as Fe-rich and Nd oxides and pores are found depending on the composition and processing parameters. Selected substituent elements replace the Nd atoms (S1 = Dy, Tb) and the Fe atoms (S2 = Co, Ni, Cr) in the hard magnetic ϕ-phase and considerably change the intrinsic properties, such as the spontaneous polarization, the Curie temperature and the magnetocrystalline anisotropy. The formation of intermetallic, soft magnetic Nd(Fe, S2) phases, such as the Laves type $Nd(Fe, S2)_2$ phase, degrade the coercivity of the magnets. If dopant elements M1 or M2 are added to Nd–Fe–B, in some cases the coercivity is increased and the corrosion resistance is improved. This is the case if the Nd-rich intergranular phase is replaced by other phases, such as $AlNd_6Fe_{13}$ and Nd_3Co. Our previous, systematic TEM studies performed on sintered, melt-spun, mechanically alloyed and hot worked magnets have shown that two different types of dopant can be distinguished independently of the processing route. The two types influence the microstructure in different ways [15, 16]:

- *Type 1 dopants* (M1 = Al, Cu, Ga)
  $\Rightarrow$ form binary M1–Nd or ternary M1–Fe–Nd phases.
- *Type 2 dopants* (M2 = Ti, Zr; V, Mo; Nb, W)
  $\Rightarrow$ form binary M2–B or ternary M2–Fe–B phases.

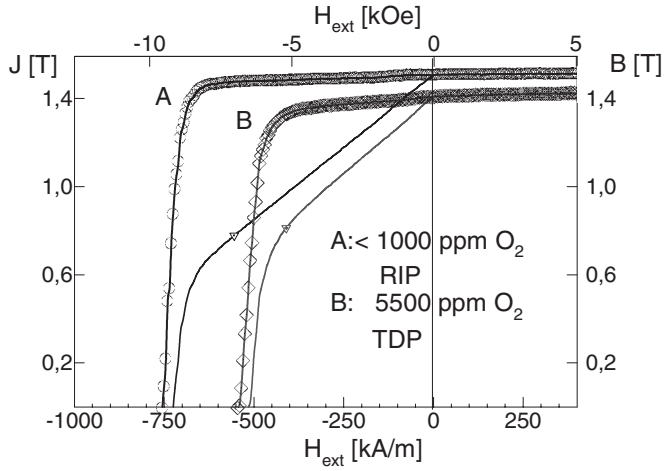

Figure 4. Comparison of demagnetization curves of $Nd_{13.5}Fe_{bal}B_{5.95}Cu_{0.03}Al_{0.7}$ sintered magnets manufactured by rubber isostatic die pressing and transverse die pressing (TDP) in air; (A) $J_r = 1.45$ T, $(BH)_{max} = 50.2$ MGOe, (B) $J_r = 1.41$ T, $(BH)_{max} = 41.9$ MGOe.

The processing route of the magnet strongly influences the grain size and grain size distribution. The coercive field in sintered magnets strongly depends on the sintering parameters, such as temperature and time. Nanocrystalline and submicron magnets are obtained by the melt-spinning route or by mechanically alloying or by the HDDR process [40, 41]. Hot pressing and die upsetting of Nd–Fe–B ribbon materials reveals a densely packed, anisotropic magnetic material. Platelet shaped grains are observed by TEM investigations. The degree of orientation of the platelets, which are stacked transverse to the press direction with the easy *c*-axis perpendicular to the face of each grain, determines the remanence and coercive field of the magnet.

Nd–Fe–B sintered magnets possessing outstanding magnetic properties have developed into a major permanent magnet material group in the 20 years since their invention. The drastic increase of the energy density product of newly developed $Nd_2Fe_{14}B$ based magnets enabled the invention of many new applications of permanent magnets. These magnets are produced by a conventional powder metallurgical process which is essentially based on alloy making, coarse milling, pulverizing, pressing in a magnetic field, sintering, heat treatment, grinding and surface coating. In this process, it is very important to keep the processing atmosphere either a vacuum or an inert gas because rare earth elements, such as Nd, Pr and Dy, which are essential for fabrication of Nd–Fe–B magnets, are easily oxidizable.

The theoretical maximum value of the energy density product is in the case of a perfectly square demagnetization curve given by

$$(BH)_{max}^{theor} = \frac{1}{4\mu_0} J_r^2 \qquad \text{if } |_J H_c| \geqslant \frac{1}{2\mu_0} J_r. \tag{2}$$

The residual flux density $B_r = J_r$ in this case is expressed by the following equation:

$$J_r = J_s \frac{\rho}{\rho_0} V_{hm} F_{hm} = J_s \frac{\rho}{\rho_0} V_{hm} \cos\varphi \tag{3}$$

where J_s is the saturation magnetization of the hard magnetic phase (1.61 T), V_{hm} and F_{hm} are the volume fraction and the degree of alignment of the hard magnetic grains, respectively. In order to enhance J_r and therefore the energy density product, it is necessary to avoid pores

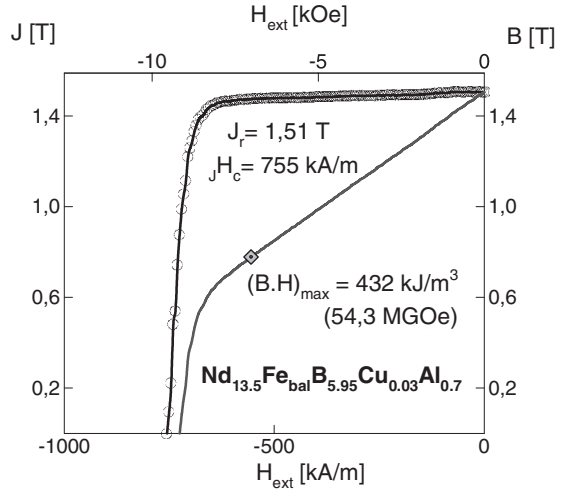

Figure 5. The demagnetization curve of an optimized high energy density sintered magnet manufactured using a combination of a rubber isostatic die and TDP.

and to densify the magnets up to the theoretical value ρ_0, increase the volume fraction $V_{\rm hm}$ and achieve a high degree of alignment $F_{\rm hm}$.

The theoretical value of the maximum energy product of $Nd_2Fe_{14}B$ based magnets is calculated to be 512 kJ m^{-3} (64 MGOe) assuming 100% perfect alignment and 100% volume fraction of the hard phase. The origin of this magnetic property lies in the $Nd_2Fe_{14}B$ ternary tetragonal compound being a main phase. In addition, according to the ternary Nd–Fe–B phase diagram this magnet also contains a certain amount of $Nd_{1.1}Fe_4B_4$ phase and an Nd-rich phase. which is essential for sintering with the liquid phase. In order to densify the magnets up to the theoretical density, it is very important to control the composition of the magnets, thus generating a sufficient amount of liquid phase upon sintering. Furthermore, controlling the volume fraction of the constituent phases is indispensable for enhancing the residual flux density ($B_{\rm r}$) and keeping the intrinsic coercivity ($_J H_{\rm c}$) stable.

Several authors have reported obtaining $Nd_2Fe_{14}B$ based magnets with energy density products >420 kJ m^{-3} [17–19] by

- keeping the oxygen content low [20];
- using the powder mixing technique [21];
- increasing the magnetizing field and reducing the pressure during compaction [22];
- using the rubber isostatic pressing (RIP) technique to improve the orientation of the particles in the green compact to obtain sintered magnets with perfect orientation.

The increasing demand for highest energy density magnets (>400 kJ m^{-3}), especially for VCM in hard disc drives and for magnetic circuits for magnetic resonance imaging devices, needs an efficient manufacturing process for $Nd_2Fe_{14}B$ sintered magnets with improved energy density products. A new technology—RIP—has been developed by Sagawa *et al* [23, 24] to improve the orientation of the particles in the green compact to obtain sintered magnets with perfect orientation. RIP is one of the key technologies approaching the theoretical limit, 64 MGOe at room temperature, of magnets based on $Nd_2Fe_{l4}B$. In RIP, magnet powder is subjected to such a strong pulsed field just before the compaction that the powder in the rubber

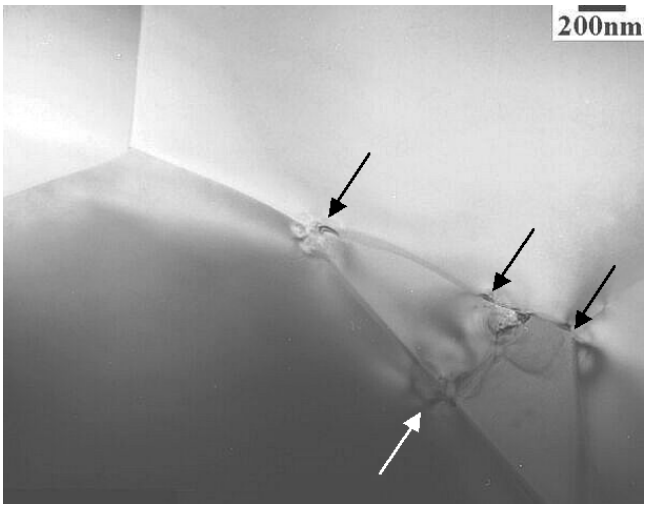

Figure 6. A TEM image of grain boundary junctions of a $Nd_{13.7}Fe_{bal}B_{5.95}Cu_{0.03}Al_{0.7}$ sintered magnet with the *c*-axis of the grains perpendicular to the image plane. Pockets of Nd-rich phases are marked by arrows.

mould is thoroughly oriented. Then the powder is compacted isostatically, while the orientation is held completely constant.

In the conventional die pressing which uses no rubber moulds, the pressure applied to the powder is uniaxial. The uniaxial pressure tends to disturb the orientation of the particles during the pressing. To prevent this orientation disturbance, the powder has to be subjected to a strong magnetic field throughout the pressing. This is one of the reasons that a pulsed field cannot be adopted for the conventional die pressing. The high orientation of the magnet produced by RIP is attributed to:

- application of a strong pulsed field which dissolves the agglomeration of the magnet powder particles and, then, impulsively orients the particles;
- isostatic pressing which holds the grain orientation constant during the pressing.

The misalignment of the hard magnetic grains with a diameter of 2–5 μm is in the best case of order $<14°$. The oxygen content of the magnets has to be reduced from values of 4000–6000 ppm to a value <1000 ppm. A high oxygen content is one limiting factor on decreasing the Nd content in order to improve the volume fraction of the hard magnetic phase. The squareness of the demagnetization curve and the coercive field drastically decrease as abnormal grain growth (AGG) of the $Nd_2Fe_{14}B$ grains occurs [25].

The remanence and energy product increase with decreasing Nd content, whereas the coercive field shows its highest value at a high Nd content. In the case where the oxygen content of the magnets was determined as of the order of 4000–6000 ppm, a large part of the Nd was bound in the stable phase Nd_2O_3. This is why below 14 at.% Nd the density and hard magnetic properties of the magnets drastically deteriorated in magnets with a high oxygen content (figure 4). In contrast, low oxygen content can cause AGG and degrade the magnetic properties. The influence of oxygen on the hard magnetic properties is more complex. Kim *et al* [26] reported that a controlled doping with oxygen improved grain alignment and resulted in an increase in remanence, coercivity and loop squareness. One possibility for improving the alignment factor is to optimize the alignment field and/or pressure during transverse pressing.

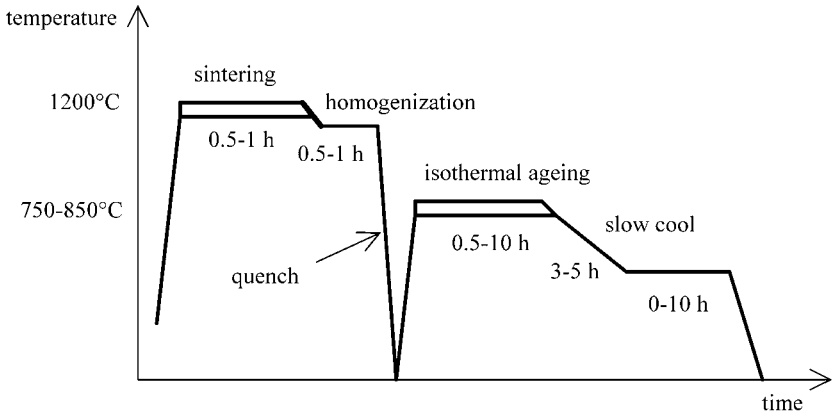

Figure 7. The schematic temperature profile for the sintering and heat treatment of a $SmCo_5/Sm_2Co_{17}$ magnet.

Even the sintering process influences the degree of alignment of the grains [27]. On the other hand, several authors [28, 24] found that isostatic die pressing ($\varphi = 11°$–$14°$) yields the highest alignment, followed by transverse field die pressing (18°–20°) and axial field die pressing (25°–27°).

Demagnetization curves for an optimized magnet with $(BH)_{max} > 430$ kJ m^{-3} and a low oxygen content and for $Nd_{13.5}Fe_{bal}B_{5.95}Cu_{0.03}Al_{0.7}$ are shown in figure 5; the corresponding TEM micrograph is shown in figure 6. The magnets produced were sintered between 960 and 1100 °C. The sintering temperature was varied to get the optimum density (7.5–7.6 g cm^{-3}) and $(BH)_{max}$. The density of the samples and the remanence increased with increasing sintering temperature, keeping the sintering time constant (3 h), while the squareness of the demagnetization curve only partly increased and drastically decreased when AGG of the $Nd_2Fe_{14}B$ grains occurred [4]. AGG of the $Nd_2Fe_{14}B$ grains occurred preferentially in magnets with low oxygen content. The oxygen content strongly affects AGG and the magnets with higher oxygen content have higher critical temperatures at which AGG occurs. Figure 6 shows that the microstructure mainly consists of $Nd_2Fe_{14}B$ grains several microns in diameter. Only a few Nd-rich phases are found as intergranular phases, especially at grain boundary junctions.

4. Pinning controlled Sm(Co, Cu, Fe, Zr)$_{7.5–8}$ magnets

$Sm(Co, Cu, Fe, Zr)_{7.5–8}$ permanent magnets are the best choice for operating temperatures above 300 °C because of the high magnetocrystalline anisotropy, the strong domain wall pinning and the high Curie temperature [11, 29, 30] of the hard magnetic phases. A complex production process (figure 7), which involves sintering, homogenizing, isothermal ageing and annealing, results in the formation of a cellular precipitation structure, which acts as pinning centres for magnetic domain walls [31]. The microstructure, which consists of the $Sm_2(Co, Fe)_{17}$ cell matrix phase, the $Sm(Co, Cu)_{5–7}$ cell boundary phase and the Zr-rich lamella phase, develops mainly during the isothermal ageing [32]. The formation of a fine cellular precipitation structure is a necessary precondition for strong magnetic properties at elevated temperatures, because the precipitates act as pinning centres for the magnetic domain walls. However, the compositions of the distinct phases and the elemental profiles have an even greater influence on the magnetic properties. The diffusional redistribution of the various elements during the heat treatment results in a characteristic microchemistry. As all of the elements are placed on regular crystallographic sites, there is only diffusion of vacancies, which

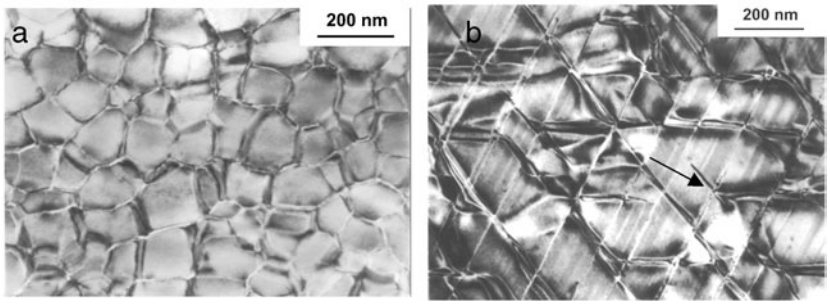

Figure 8. TEM micrographs showing typical, rhombic, cellular precipitation structures of a sintered $SmCo_5/Sm_2Co_{17}$ magnet for high temperature applications. Views (a) parallel and (b) perpendicular to the alignment direction (→).

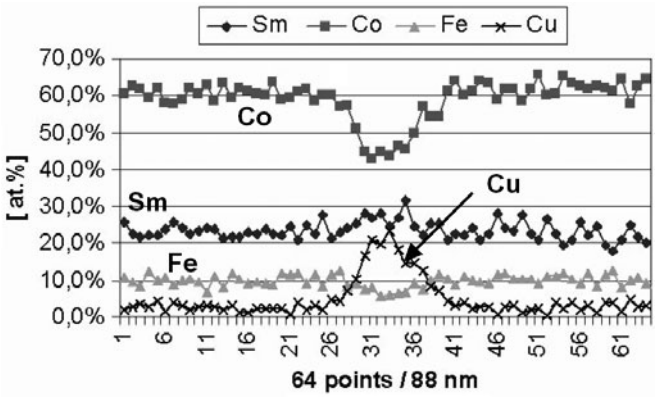

Figure 9. Elemental TEM nanoprobe profiles across a cell boundary phase.

is very slow compared to interstitial diffusion. There are two main diffusional processes: Cu segregates to the 1:5 cell boundary phase and Fe segregates to the 2:17 matrix phase. As the cell size of the precipitation structure increases with the duration of the isothermal ageing, it is necessary to decrease the temperature when the desired cell size has been obtained. Diffusion continues during the following slow cooling and the subsequent annealing at 400 °C, but with a reduced rate because of the lower temperatures. Even the solutionized samples may have a microstructure and microchemistry which have a strong influence on the duration and the profile of the heat treatment. Tang *et al* [33] reported Cu clusters within the solid solution which enabled a higher Cu diffusion rate and allowed the samples to be quenched directly after the isothermal ageing.

The TEM micrographs of figure 8 show the typical cellular and lamellar precipitation structures and figure 9 is a typical EDX line-scan across a cell boundary phase taken with a high resolution TEM equipped with a field emission gun (FEG) in the nanoprobe mode. The Fe content within the cell matrix phase is always higher than the nominal content, which confirms that Fe mainly segregates to the 2:17 phase. A higher Fe/Co ratio decreases the anisotropy constant K_1 [34] and increases the spontaneous magnetization M_s [35]. The Zr content within the cell matrix phase lies between 1.0 and 2.4 at.%. Because of the low Zr concentration, a detailed analysis would require longer measurement times in order to achieve a better signal to noise ratio. Nevertheless the data reveal that the Zr content within the 2:17 phase is higher than expected [36, 37]. A high Zr concentration is found in the platelet phase perpendicular

to the c-axis, which presumably acts as diffusion path for the distribution of elements during the annealing procedure.

The cellular $Sm(Co, Cu)_{5-7}$ precipitation structure acts as pinning centres for the magnetic domain walls. The coercivity is determined by the difference in and the gradient of the domain wall energy. The exchange constant A and the anisotropy constant K_1 of the cell boundary phase are mainly determined by the Cu concentration [38]. The investigations reveal that, in general, the Cu concentration is rather low, resulting in a repulsive pinning coercivity mechanism [39]. The Cu content in the 1:5 phase should be as low as possible or as high as necessary to make the 1:5 phase non-ferromagnetic. In low Cu samples the K_1 values of the 1:5 and the 2:17 phases cross at a certain temperature, which does not happen in high Cu samples. However, as a large part of the magnet consists of the 1:5 phase, the spontaneous magnetization M_s is strongly decreased in high Cu samples. The actual domain wall pinning process is rather complicated and varies from repulsive to attractive, depending on whether the magnetocrystalline anisotropy in the Cu containing 1:5 cell boundary phase is lower or higher than in the 2:17 cell matrix phase, respectively. The shape and the thickness of the cell boundary phase and the elemental profiles across the phase determine the coercivity H_c.

Recently a new series of magnets with H_c up to 1050 kA m^{-1} at 400 °C has been developed [29]. These magnets have low temperature coefficients of H_c and a straight line B versus H (extrinsic) demagnetization curve up to 550 °C. High Cu, low Fe and a higher Sm concentration were found to contribute to high coercivity at high temperatures.

5. Nanocrystalline, composite $Nd_2Fe_{14}B/(\alpha$-Fe, $Fe_3B)$ and other novel rare earth magnets

The increasing demand for powders for bonded magnets led to the development of nitrided Sm–Fe and nanocrystalline Nd–Fe–B materials. The RE_2Fe_{17} compounds have low Curie temperatures and exhibit planar magnetic anisotropy. Substitutions or additions are needed to raise T_C and to change the magnetocrystalline anisotropy. Almost any substitution will raise T_C, but recent attention has focused on Al and Ga which also induce uniaxial anisotropy when present in modest amounts in Sm_2Fe_{17}. However, the most effective way of increasing T_C for R_2Fe_{17} and modifying its anisotropy is to use interstitial additions (B, C, N). Interstitial modification, especially with nitrogen, has added a new dimension to the compounds that can be considered from the rare earth permanent magnets. Besides raising T_C for iron-rich intermetallics, largely through the effect of lattice expansion (6%), interstitial atoms also control the magnetocrystalline anisotropy. Since 1990, there have been extensive studies of interstitial 2:17, 3:29 and 1:12 compounds containing nitrogen and carbon in the structures, but the interstitial compound which exhibits the most favourable combination of intrinsic magnetic properties remains $Sm_2Fe_{17}N_{3-x}$ with $T_C = 470$ °C. Mechanical alloying and HDDR of $Sm_2Fe_{17}N_3$ give high coercivity and good loop shape, but have so far only yielded isotropic material. The main disadvantage of nitrided powders is the dissociation at high temperature (about 600 °C) according to the reaction

$$Sm_2Fe_{17}N_3 \rightarrow 2SmN + Fe_4N + 13\alpha\text{-Fe}.$$

Another useful family are the pseudo-binaries $Sm(Fe_{12-x}M_x)$ where M = Ti, V, Si, ... which crystallize in the tetragonal $ThMn_{12}$ structure [42]. The best of them show T_C and magnetic anisotropy similar to those of $Nd_2Fe_{14}B$, but with somewhat lower magnetization. These compounds can also be improved by interstitial modification with nitrogen or carbon.

Nanocrystalline, single phase $Nd_2Fe_{14}B$ magnets with isotropic alignment show an enhancement of remanence which is attributed to intergrain exchange interactions, which enhance the remanence by more than 40% as compared to the remanence of non-interacting

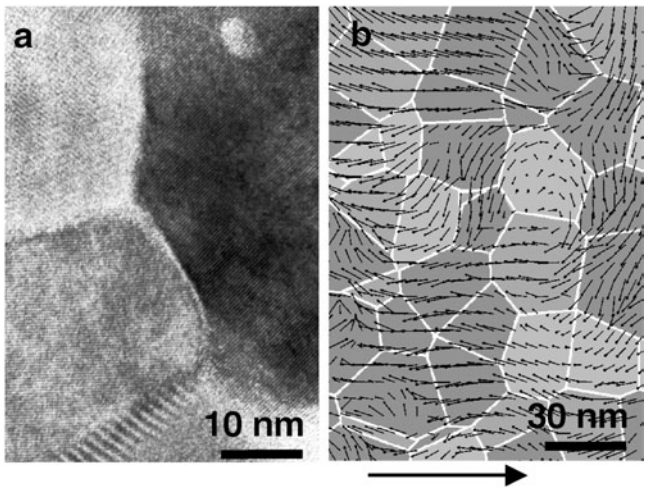

Figure 10. (a) A high resolution electron micrograph of a nanocrystalline, single phase Nd–Fe–B magnet with isotropic alignment. (b) The calculated magnetization distribution with a vortex-like structure in a slice plane of a 40 vol% $Nd_2Fe_{14}B$, 30 vol% α-Fe and 30 vol% Fe_3B magnet with a mean grain size of 30 nm for zero applied field. The magnetic polarization remains parallel to the saturation direction (arrow) within the soft magnetic grains, whereas it rotates towards the direction of the local anisotropy direction within the hard magnetic grains.

particles, if the grain size is of the order of 10–30 nm (figure 10(a)). Numerical micromagnetic calculations have revealed that the interplay of magnetostatic and exchange interactions between neighbouring grains influences the coercive field and remanence considerably [43]. After saturation, the three-dimensional micromagnetic simulation shows a large volume fraction of an inhomogeneous polarization distribution near grain boundaries in small grained isotropic, single phase magnets, leading to an increase of the remanence and a decrease of the coercive field. Exchange interactions between neighbouring soft and hard grains lead to remanence enhancement of isotropically oriented grains in nanocrystalline, two phase, composite magnets [44–49]. Soft magnetic grains in two phase or multiphase, composite, permanent magnets cause high polarization and hard magnetic grains induce a large coercive field provided that the particles are small and strongly exchange coupled. The coercive field shows a maximum at an average grain size of 15–20 nm. Intergrain exchange interactions override the magnetocrystalline anisotropy of the $Nd_2Fe_{14}B$ grains for smaller grains, whereas exchange hardening of the soft phases becomes less effective for larger grains. The magnetization distribution at zero applied field for different grain sizes clearly shows that the remanence enhancement and energy product increase with decreasing grain size and increase with increasing α-Fe content. Owing to the competitive effects of magnetocrystalline anisotropy and intergrain exchange interactions, the magnetization of the hard magnetic grains significantly deviates from the local easy axis for a grain size $D \leqslant 20$ nm. As a consequence coercivity drops, since intergrain exchange interactions help to overcome the energy barrier for magnetization reversal. With increasing grain size the magnetization becomes non-uniform, following either the magnetocrystalline anisotropy direction within the hard magnetic grains or forming a flux closure structure in soft magnetic regions. Neighbouring α-Fe and Fe_3B grains may make up large continuous areas of soft magnetic phase, where magnetostatic effects will determine the preferred direction of the magnetization. The large soft magnetic regions degrade the squareness of the demagnetization curve and cause a decrease of the coercive field for $D > 20$ nm. A vortex-like magnetic state with vanishing net magnetization will form

within the soft magnetic phase if the diameter of the soft magnetic region exceeds 80 nm. Figure 10(b) presents the calculated magnetization distribution in a slice plane of a 40 vol% $Nd_2Fe_{14}B$, 30 vol% α-Fe and 30 vol% Fe_3B magnet with a mean grain size of 30 nm for zero applied field. The magnetic polarization remains parallel to the saturation direction within the soft magnetic grains, whereas it rotates towards the direction of the local anisotropy direction within the hard magnetic grains.

Many of the fully dense permanent magnet materials, especially those that are sintered, are very hard and brittle and machining them to their final shape is often tedious. The reduction of production handling and assembly costs led to an interest in *bonded* magnets, which are made by consolidating a magnet powder with a polymer matrix. While machining is easy, the production processes also frequently allow parts to be made directly at their final dimensions. Thermosetting binders such as epoxy resin are employed for use in compression-moulded magnets, thermoplastic binders such as nylon for use in injection-moulded magnets and elastomers such as rubber for use in extruded magnets [50]. The major drawback to bonded magnets is the reduction in their magnetic properties, relative to those that are 100% dense with magnetic material.

6. Summary

Microstructural parameters, such as grain size, shape of grains, crystal structure, crystal defects, orientation and composition of the various phases, are different in $SmCo_5$, Sm_2Co_{17} and $Nd_2Fe_{14}B$ based permanent magnet materials. The complex microstructure considerably influences the magnetic reversal process. Detailed TEM analysis revealed various additional binary and ternary phases in the intergranular region between hard magnetic grains in doped and substituted Nd–Fe–B magnets. Intergranular phases change the behaviour of the coupling between the hard magnetic grains. Non-magnetic phases eliminate the direct exchange interaction and also reduce the long range magnetostatic coupling between the hard magnetic grains; both effects lead to an increase of the coercive field. The Nd-rich intergranular phase is necessary for the liquid phase sintering process, but degrades the corrosion stability and reduces the remanence. In order to the improve coercive field, remanence and energy density, it is necessary to increase the volume fraction of the hard magnetic phase by decreasing the amount of oxygen, neodymium and pores and to improve the degree of alignment of the $Nd_2Fe_{14}B$ grains. Oxygen is partly dissolved in the Nd-rich intergranular phase. On reducing the amount of oxygen ($<$1000 ppm) the problem of AGG during sintering becomes more severe. The difference in magnetic domain wall energy in precipitation hardened magnets $Sm(Co, Cu)_5/Sm_2(Co, Fe)_{17}$ multiphase magnets is the main factor determining the coercive field. The inhomogeneous magnetization behaviour near the intergranular regions of nanocrystalline rare earth magnets, which is directly responsible for remanence and coercivity, is strongly influenced by the microstructural parameters.

Acknowledgments

This work was partly supported by the EC project HITEMAG (GRD1-1999-11125) and by the FWF project P14899-N02.

References

[1] Becker J, Luborsky F E and Martin L M 1968 *IEEE Trans. Magn.* **4** 84
[2] Coey J M D 1995 *J. Magn. Magn. Mater.* **140–144** 1041
[3] Stadelmaier H H, Henig E T and Petzow G 1991 *Z. Metallk.* **82** 163
[4] Livingston J D 1996 *MRS Bull.* **4** 55
[5] Strnat K J, Hoffer G, Oson J and Ostertag W 1967 *J. Appl. Phys.* **38** 1001

[6] Sagawa M, Fujimura S, Togawa N, Yamamoto H and Matsuura Y 1984 *J. Appl. Phys.* **55** 2083
[7] Croat J J, Herbst J F, Lee R W and Pinkerton F E 1984 *J. Appl. Phys.* **55** 2078
[8] Herbst J F and Croat J J 1991 *J. Magn. Magn. Mater.* **100** 57
[9] Fidler J and Schrefl T 2000 *J. Phys. D: Appl. Phys.* **33** R135
[10] Hadjipanayis G C, Hazleton R C and Lawless K R 1984 *J. Appl. Phys.* **55** 2073
[11] Strnat K J 1988 Rare earth–cobalt permanent magnets *Ferromagnetic Materials* vol 4 (Amsterdam: Elsevier) p 131
[12] Herbst J F 1991 *Rev. Mod. Phys.* **63** 819
[13] Mishra R K 1987 *J. Appl. Phys.* **62** 967
[14] Fidler J and Schrefl T 1996 *J. Appl. Phys.* **79** 5029
[15] Bernardi J, Fidler J and Foedermayr F 1992 *IEEE Trans. Magn.* **28** 2127
[16] Bernardi J and Fidler J 1994 *J. Appl. Phys.* **76** 6241
[17] Kaneko Y 2000 *IEEE Trans. Magn.* **36** 3275
[18] Fidler J, Sasaki S and Estevez-Rams E 1999 *Advanced Hard and Soft Magnetic Materials* (*Mater. Res. Soc. Symp. Proc.* vol 577) (Warrendale, PA: Materials Research Society) p 291
[19] Rodewald W, Wall B, Katter M and Uestuener K 2002 *IEEE Trans. Magn.* **38** 2955
[20] Sagawa M, Hirosawa S, Yamamoto H, Fujimura S and Matsuura Y 1987 *Japan. J. Appl. Phys.* **26** 785
[21] Otsuki E, Otsuka T and Imai T 1990 *Proc. 11th Int. Workshop on Rare Earth Magnets and their Applications (Pittsburgh, PA, 1990)* vol 1, ed S G Shankar p 328
[22] Endoh M and Shindo M 1994 *Proc. 13th Int. Workshop on Rare Earth Magnets and their Applications (Birmingham, UK, 1994)* vol 1, ed C A F Manwaring, D G F Jones, A J Williams and I R Harris p 397
[23] Sagawa M and Nagata H 1993 *IEEE Trans. Magn.* **29** 2747
[24] Sagawa M, Nagata H, Itatani O and Watanabe W 1994 *Proc. 13th Int. Workshop on Rare Earth Magnets and their Applications (Birmingham, UK, 1994)* ed C A F Manwaring, D G F Jones, A J Williams and I R Harris Suppl. 13
[25] Rodewald W, Wall B and Fernengel W 1997 *IEEE Trans. Magn.* **33** 3841
[26] Kim A S, Camp F E and Stadelmaier H H 1994 *J. Appl. Phys.* **76** 6265
[27] Chin T S, Hung M P, Tsai D S, Wu K F and Chang W C 1988 *J. Appl. Phys.* **64** 5531
[28] Fernengel W, Lehnert A, Katter M, Rodewald W and Wall B 1996 *J. Magn. Magn. Mater.* **157/158** 19
[29] Chen C H, Walmer M S, Walmer M H, Liu S, Kuhl G E and Simon G K 1998 *J. Appl. Phys.* **83** 6706
[30] Hadjipanayis G C, Tang W, Zhang Y, Chui S T, Liu J F, Chen C and Kronmuller H 2000 *IEEE Trans. Magn.* **36** 3382
[31] Fidler J 1982 *J. Magn. Magn. Mater.* **30** 58
[32] Fidler J, Skalicky P and Rothwarf F 1983 *IEEE Trans. Magn.* **19** 2041
[33] Tang W, Zhang Y, Goll D, Hadjipanayis G C and Kronmuller H 2001 *J. Magn. Magn. Mater.* **226–230** 1365
[34] Perkins R S and Straessler S 1977 *Phys. Rev.* B **15** 477
[35] Perkins R S and Straessler S 1977 *Phys. Rev.* B **15** 490
[36] Ray A E 1984 *J. Appl. Phys.* **55** 2094
[37] Ray A E 1990 *J. Appl. Phys.* **67** 4972
[38] Lectard E, Allibert C H and Ballou R 1994 *J. Appl. Phys.* **75** 6277
[39] Fidler J, Matthias T, Scholz W, Schrefl T, Rong T S, Jones I and Harris I R 2002 *Proc. 17th Rare Earth Magnets Workshop (Newark, DE, 2002)* ed G Hadjipanayis and M J Bonder p 853
[40] Harris I R 1992 *Proc. 12th Int. Workshop on Rare Earth Magnets and their Applications (The University of Western Australia, Perth, Australia, 1992)* ed B Street p 347
[41] Nakayama R, Takeshita T, Itakura M, Kuwano N and Oki K 1994 *J. Appl. Phys.* **76** 412
[42] Buschow K H J 1988 Permanent magnet materials based on 3d-rich ternary compounds *Ferromagnetic Materials* vol 4, ed E P Wohlfarth and K H J Buschow (Amsterdam: Elsevier) p 1
[43] Schrefl T and Fidler J 1999 *Advanced Hard and Soft Magnetic Materials* (*Mater. Res. Soc. Symp. Proc.* vol 577) (Warrendale, PA: Materials Research Society) p 163
[44] Kneller E F and Hawig R 1991 *IEEE Trans. Magn.* **27** 3588
[45] Davies H A, Manaf A, Leonowicz M, Zhang P Z, Dobson S J and Buckley R A 1993 *Nanostructured Materials* vol 2 (Oxford: Pergamon) p 197
[46] McCallum R W, Kadin A M, Clemente G B and Keem J E 1987 *J. Appl. Phys.* **61** 3577
[47] Coehoorn R, Mooij D B and Waard C D E 1989 *J. Magn. Magn. Mater.* **80** 101
[48] Hadjipanayis G C and Gong W 1988 *J. Appl. Phys.* **64** 5559
[49] Ding J, McCormick P G and Street R 1993 *J. Magn. Magn. Mater.* **124** 1
[50] Campbell P 1994 *Permanent Magnet Materials and their Applications* (Cambridge: Cambridge University Press)